

1. INTRODUCTION:

In mountainous regions, landsliding is an important source of damage and fatalities which correlates with extreme rainfall events (Kirschbaum et al., 2012) and may increase with climate change (Gariano and Guzzetti, 2016, Fig 1).

Still, how precipitation controls landsliding is poorly understood quantitatively, especially at the scales of large and extreme rainfall events. Mechanistic models coupling water infiltration to slope stability exist (Iverson, 2000), but are not yet operational at the regional scale because of the difficulty to constrain key parameters. Current empirical studies constrain only the minimum rainfall for landslide occurrence (Fig 1).

An alternative is to constrain empirically the relation between rainfall and several landslide metrics representing proxies of landslide intensity. This requires simultaneous characterization of rainfall and landsliding for a large number of rainfall events, at sufficiently high spatio-temporal resolution.

Combining multiple satellite dataset is a plausible way to address these issues.

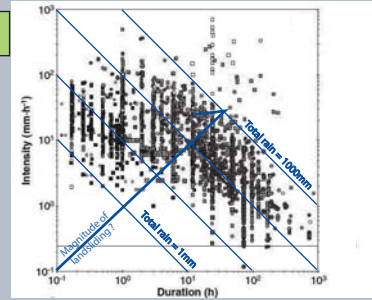


Figure 1 : Intensity duration thresholds for landslide occurrence based on a global compilation (Modified after Guzzetti et al., 2008). Such approach do not consider landslide magnitude and its relation with intensity, duration or total rainfall.

2. DATA : GLOBAL COMBINATION OF RAINFALL ESTIMATES AND LANDSLIDE INVENTORIES

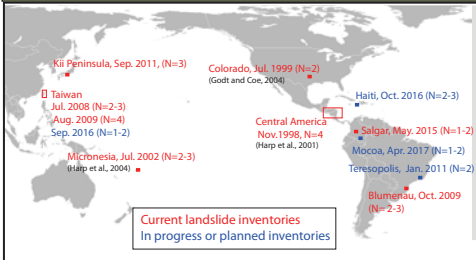


Figure 2 : Summary of locations where landslide inventories (mapped as polygons) associated with a single storm are available. N indicates the order of magnitude of landslide number during the event (i.e., N=2 ~100 landslides). Unreferenced inventories are from this work.

Topographic indexes: Global 30m-SRTM DEM is converted into 1km² cells within which the modal slope is computed. Only cells >10° are considered prone to landsliding.

Rainfall estimates
In this work we compared unaged multi-satellite products TRMM-3b42-v7 and GSMaP-MVK-6.5, the MSWEP-v2 (Beck et al., 2017) product combining satellite, gages and model reanalysis to in-situ rain gages network and soon to in-situ weather radar data for Brasil.

Landslide maps:

Based on man-made interpretation of airphotos or satellite imagery, allowing to map every resolvable landslide in the area of occurrence of the storm. Polygons allow to study not only number, but size distribution, shapes, areas and volumes.

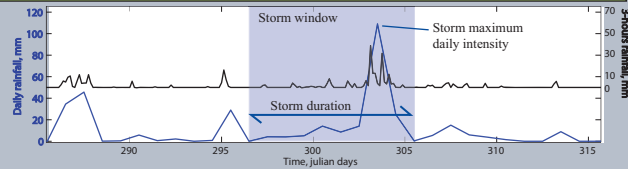


Figure 3 : TRMM - 3b42 estimated rainfall during hurricane Mitch (1998) at Lat = 13.125° and Lon = -88.625°. The storm window is defined as the interval between closest dry days (rainfall <= 1 mm) bracketing the maximum intensity. This window is used to define duration, total rainfall and mean storm intensity at the daily scale. 3-hourly (TRMM) or hourly (GSMaP) may be used to better characterized mean and maximum rainfall intensities. Antecedent rainfall may also be considered as an additional parameter.

3. RAINFALL PRODUCTS VALIDATION : THE IMPORTANCE OF OROGRAPHIC RAINFALL

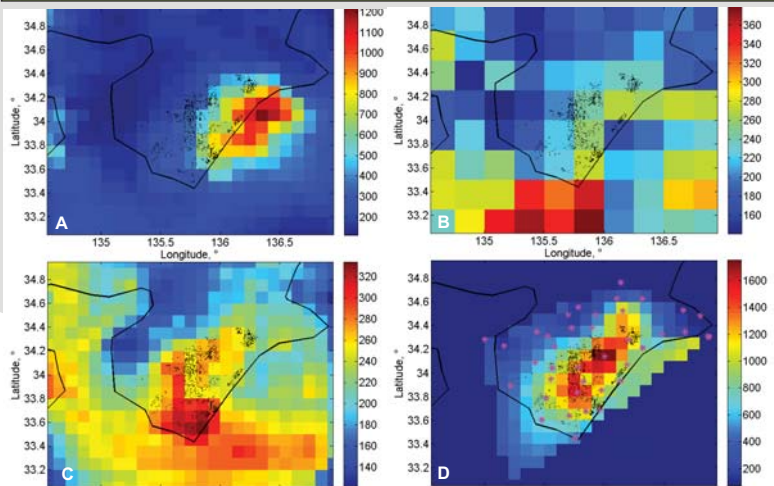


Figure 4 : Total rainfall (in mm) due to Typhoon Talas (6-9-Sep-2011) in Japan, estimated by GSMaP (A), TRMM (B), MSWEP (C) and a local gage network (D). Note the different rainfall scale. Gages locations are noted with pink stars and landslides that occurred during the storm are black dots.

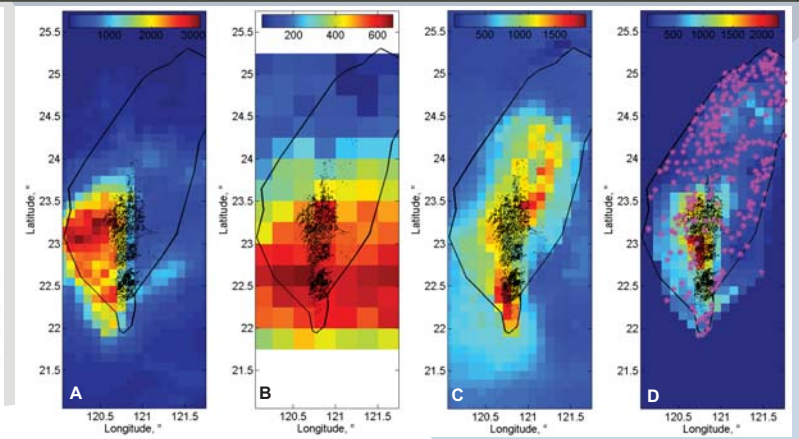


Figure 5 : Same as Figure 4, for the total rainfall (in mm) due to Typhoon Morakot (7-10-Aug-2009) in Taiwan.

Orographic rainfall is a dominant process in many cases of rainfall induced landslides (Fig 4,5)

It is not detected by TRMM or MSWEP products. GSMaP retrieves heavy rain but with some over-estimation and some mislocation. Still it may be useful for early warning.

4. RAINFALL-LANDSLIDE SCALING : THE IMPORTANCE SOIL DYNAMICS

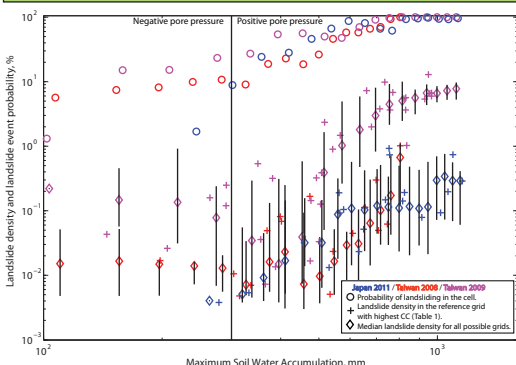


Figure 6 : Landslide density (total area in the cell divided by area in the cell where slope exceeds 15°) and probability of landsliding in the cell VS modelled maximum soil water accumulation (Wilson and Wiczorek 1995) for a 2m regolith, evapotranspiration rate of 3mm/day, total and drained porosity of 0.35 and 0.2, and a drainage coefficient of 0.02 and 0.005 for Japan and Taiwan, respectively.

METHODS:

In each gridcell (0.2x0.2°) where topography is not null, we estimate average rainfall and landslide parameters (Rp and Lp, respectively).

Given that the gradient in both rainfall and landslide properties are much finer than the grid resolution, cell properties and spatial correlation will vary with the grid coordinates. To obtain an objective scaling, we compute Rp and Lp for 100 different grids (incremental horizontal and vertical shifts), and derive 16th, 50th and 84th percentiles of Lp within bins or Rp (Figure 6). This constrain the probabilistic magnitude of a given rainfall estimated on a randomly chosen grid. We also constrain the probability of having any landsliding for a given Rp, based on the number of gridcell where landslides occur or not.

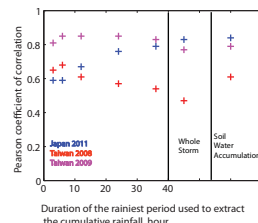


Figure 7 : Pearson coefficient of correlation between the logarithm of the landslide density and the logarithm of the total rainfall during the rainiest period of different duration, or the soil accumulation model.

Coefficient are for all reference grids. The different event are dominated by different timescales that are retrieved by the soil model.

CONCLUSIONS

Orographic rainfall matters! It is currently partially captured by GsMAP-RT (Fig 4, 5). Satellite products are not ready yet for a spatial forecast of landsliding.

However, coupling rainfall history from gages with a **simple subsurface hydrological model** yield a **unique behavior for several typhoons** (Fig 6) that otherwise would require to consider different timescale for rainfall accumulation (Fig 7). All cases behave with a **threshold** above which landslide event probability and landslide density increase non-linearly with the **maximum soil water content**. Some phenomenon of **saturation**, possibly related to **hortonian flow** may have to be considered in the typhoons in Japan (2011) and in Taiwan (2009) (Fig 6).

Additional analysis on other cases (Brasil, Haiti) will allow to test the robustness of this global approach.

Acknowledgments:

I am funded by the CNES through a post-doctoral scholarship. This study also integrate into the CEOS Landslide Pilot project. We thanks NASA and JAXA for providing rainfall estimates from the TRMM and GSMaP algorithms.

REFERENCES:

- Beck, H. E., van Dijk, A. J. J. M., Levizzani, V., Schellekens, J., Miralles, D. G., Martens, B., & de Roo, A. (2017). MSWEP: 3-hourly 0.25° global gridded precipitation (1979-2015) by merging gauge, satellite, and reanalysis data. *Hydro. Earth Syst. Sci.*, 21(1), 589-615.
- Gariano, S. L., and F. Guzzetti (2016). Landslides in a changing climate. *Earth-Science Reviews*.
- Godt, J. W., and J. A. Coe (2007). Alpine debris flows triggered by a 28 July 1999 thunderstorm in the central Front Range, Colorado. *Geomorphology*, 84(1-2), 80-97.
- Guzzetti, F., S. Ferencacci, M. Rossi, and C. P. Stark (2008). The rainfall intensity-duration control of shallow landslides and debris flows: an update. *Landslides*, 5(1), 3-17.
- Harp, E. L., M. E. Reid, and J. A. Michael (2004). Hazard analysis of landslides triggered by Typhoon Chata on July 2, 2002, in Chuuk State, Federated States of Micronesia. Open-File Report, USGS.
- Harp, E. L., K. W. Hagan, M. D. Held, and J. P. McKenna (2002). Digital inventory of landslides and related deposits in Honduras triggered by Hurricane Mitch. Open-File Report, USGS.
- Iverson, R. M. (2000). Landslide triggering by rain infiltration. *Water Resour. Res.*, 36(7), 1897-1910.
- Kirschbaum, D., R. Adler, C. Peters-Lidard, and G. Huffman (2012). Global Distribution of Extreme Precipitation and High-Impact Landslides in 2010 Relative to Previous Years. *J. Hydrometeorol.*, 13(5), 1536-1551.
- Wilson, R. C., & Wiczorek, G. F. (1995). Rainfall Thresholds for the Initiation of Debris Flows at La Honda, California. *Environmental & Engineering Geoscience*, 1(1), 11-27.